OPTIMIZED RESIDUAL IMAGE FOR STEREO IMAGE CODING

Walid Hachicha [1], *Mounir Kaaniche* [1], *Azeddine Beghdadi* [1], *Faouzi Alaya Cheikh* [2]

[1]L2TI, Institut Galilée, Université Paris 13, Sorbonne Paris Cité, France
[2]The Norwegian Colour and Visual Computing Lab, Gjøvik University College, Norway
walid.hachicha@univ-paris13.fr, mounir.kaaniche@univ-paris13.fr, azeddine.beghdadi@univ-paris13.fr, faouzi.cheikh@hig.no

ABSTRACT

Many research works have been developed for stereo image compression purpose by focusing on the disparity compensation technique. For this reason, a great attention should be paid to the generation of the disparity-compensated residual image. Generally, the residual image is computed through a simple substruction of the disparity-compensated reference image from the target one. In this paper, we investigate two techniques for optimizing the computation of the residual image. The obtained results confirm the benefits of these optimization approaches in the context of stereo image coding.

Index Terms— Stereo image, compression, disparity compensation, optimization, ℓ_2 and ℓ_1 minimization.

1. INTRODUCTION

Stereoscopic imaging has gained a growing interest in many emerging applications such as 3D TV, 3D Digital cinema, immersive games and videoconferencing. The main advantage of stereoscopic technology is that it enhances the depth perception and makes the 3D experience more vivid. This technology requires the acquisition of two images, called left and right images, by recording two slightly different views angles of the same scene. Thus, adding the third dimension to the viewer/player leads to the doubling of the image data size compared to the monoscopic case, and consequently, involves a large amounts of stereo data. Therefore, it becomes necessary to design efficient stereo compression techniques for storing and transmitting purpose.

To this end, the simplest way for compressing stereo image (SI) is the independent coding scheme where the left and right images are encoded separately by using existing still image coders. However, since these images result from the projection of the same 3D scene and so present similar visual contents, it has been shown that more efficient joint coding schemes can be developed by taking into account the inter-image redundancies. More precisely, the common idea behind most of the existing methods is based on the following steps [1, 2]:

① First, one image is selected as a reference image (for example the left one).

② Then, the disparity map, representing the displacement field between the pixels of the right and left images, is often estimated using a block-based approach.

③ After that, the right view, referred to as target image, is predicted from the reference one using the estimated disparity map, and the difference between the original target image and the predicted one, called residual image, is generated.

④ Finally, the reference and residual images as well as the disparity map are encoded.

While the disparity map is often losslessly encoded using a DPCM technique, the reference and residual images can be encoded in different transform domains [3–6].

Therefore, the third step related to the generation of the residual image plays a key issue in the design of an efficient joint stereo image compression scheme. Most of the reported methods apply a simple subtraction between each pixel of the target image and its homologous one in the reference image. In order to better exploit the inter-view dependencies, we propose in this paper to use the neighborhood of the homologous pixel to predict the pixel of the target image. To this end, we investigate two minimization techniques, based on the use of ℓ_2 and ℓ_1 criteria, for optimizing the generation of the residual image. Note that the benefits of such optimization criteria have been recently shown in the context of the design of lifting operators in a wavelet-based coding scheme [7].

The rest of this paper is organized as follows. In Section 2, the disparity compensation technique for stereo image coding is presented. The developed optimization techniques for generating the residual image are described in Section 3. In Section 4, experimental results are given and conclusions are drawn in Section 5.

2. DISPARITY COMPENSATED RESIDUAL CODING

Stereo matching algorithms consist of assigning to each pixel of the target image $I^{(r)}$ a displacement value that allows to find its homologous point in the reference image $I^{(l)}$. Such problem has been extensively studied in computer vision, and a review of disparity estimation techniques can be found in

[8]. In the context of stereo image coding, block-matching algorithms are often used because all pixels belonging to the same block can be represented by only one value, and so requires a few bits to encode the resulting disparity map. More precisely, after partitioning the target image into non-overlapping blocks, the disparity value associated to each block is obtained by minimizing a similarity criterion $\mathcal{D}$ as follows:

$$d = \underset{d_0 \in \{1,\ldots,d_{max}\}}{\arg\min} \mathcal{D}\big(I^{(r)}(i,j), I^{(l)}(i+d_0,j)\big), \quad (1)$$

where (i,j) are the spatial coordinates of the top left pixel in the block, and d_{max} represents the potential maximum disparity value. In general, the similarity criterion is the sum of square difference (SSD) or the sum of absolute difference (SAD).
Once the disparity map is estimated, the target image $I^{(r)}$ can be predicted by shifting the reference image $I^{(l)}$ along the horizontal direction thanks to the disparity information. Then, the residual image $I^{(e)}$ is generated as follows:

$$I^{(e)}(i,j) = I^{(r)}(i,j) - I^{(l)}(i+d(i,j),j), \quad (2)$$

Thus, the reference image, the residual one and the disparity map are encoded and transmitted to the decoder side. Note that the reconstruction of the stereo images from these data is straightforward. Indeed, the reference and residual images as well as the disparity map are firstly decoded. Then, the target image is predicted using the decoded reference image and the disparity information. Finally, the target image is reconstructed by adding the decoded residual image to the predicted target one.

3. OPTIMIZED RESIDUAL IMAGE

3.1. Motivation and computation strategy

Although most of the reported stereo image coding methods generate the residual image according to Eq. (2), it is worth pointing out that this computation strategy may be suboptimal. Indeed, some authors have proposed to weight the compensation term to take into account the illumination variation between the two views [9]:

$$I^{(e)}(i,j) = I^{(r)}(i,j) - \alpha I^{(l)}(i+d(i,j),j), \quad (3)$$

where $\alpha \in \mathbb{R}_+^*$.
Most importantly, the homologous pixel $I^{(l)}(i+d(i,j),j)$ may not appear exactly on the epipolar line due to the presence of noise, the numerical rectification error, and the deviation from the pinhole camera model. Therefore, during the subtraction (i.e prediction) operation, instead of only taking the homologous pixel $I^{(l)}(i+d(i,j),j)$, it becomes more interesting to use also its neighboring samples. More precisely, we will consider the following equation for computing the residual image:

$$I^{(e)}(i,j) = I^{(r)}(i,j) - \mathbf{p}^\top \mathbf{I}^{(c)}(i,j), \quad (4)$$

where

$$\mathbf{I}^{(c)}(i,j) = \Big(I^{(l)}(i+d(i,j)+m, j+n)\Big)_{\substack{-M/2 \le m \le M/2 \\ -N/2 \le n \le N/2}} \quad (5)$$

is the vector, of dimension $(M+1)\times(N+1)$, containing the pixels of the left image used in the prediction step, and $\mathbf{p}$ is the prediction vector.
Once the computation strategy of the residual image is described, we focus now on the optimal design of the vector $\mathbf{p}$. The objective is to produce a compact representation of the residual image by minimizing a given cost functional $\mathcal{J}$:

$$\mathbf{p}^{\text{opt}} = \underset{\mathbf{p}\in\mathbb{R}^L}{\arg\min}\, \mathcal{J}(\mathbf{p}), \quad (6)$$

where $L = (M+1)\times(N+1)$.
In what follows, two minimization criteria will be investigated.

3.2. ℓ_2 optimization technique

Since the residual image corresponds to a prediction error, the vector of the prediction weights can be optimized by minimizing the variance of the residual coefficients (i.e their ℓ_2-norm). Thus, the corresponding criterion is expressed as follows:

$$\mathcal{J}(\mathbf{p}) = \sum_{i=1}^{W}\sum_{j=1}^{H}\Big(I^{(r)}(i,j) - \mathbf{p}^\top \mathbf{I}^{(c)}(i,j)\Big)^2, \quad (7)$$

where W and H are the width and the height of the stereo images.
By minimizing this criterion, it can be checked that the optimal prediction vector $\mathbf{p}^{\text{opt}}$ must satisfy the well-known Yule-Walker equations:

$$\mathsf{E}[\mathbf{I}^{(c)}(i,j)\mathbf{I}^{(c)}(i,j)^\top]\mathbf{p}^{\text{opt}} = \mathsf{E}[I^{(r)}(i,j)\mathbf{I}^{(c)}(i,j)], \quad (8)$$

where $\mathsf{E}[\cdot]$ denotes the mathematical expectation.

3.3. ℓ_1 optimization technique

Sparse representations have attracted a great deal of attention in many application fields during the last years such as compressive sensing, image debluring and image compression [7, 10]. Therefore, with the ultimate aim of increasing the sparsity of the residual coefficients, we propose to study also an ℓ_1 optimization technique for designing the optimal prediction vector. More precisely, the objective consists in minimizing the following ℓ_1 criterion:

$$\mathcal{J}(\mathbf{p}) = \sum_{i=1}^{W}\sum_{j=1}^{H}|I^{(r)}(i,j) - \mathbf{p}^\top \mathbf{I}^{(c)}(i,j)|. \quad (9)$$

It should be noted that the sparsest residual coefficients could be obtained by minimizing an ℓ_0 criterion. However, such a problem is inherently non convex and NP-hard. For this reason, we have focused on the use of ℓ_1 criterion which is convex and can be efficiently solved thanks to a class of proximal optimization algorithms [11]. Among them, we adopt the Douglas-Rachford algorithm which was found to be simple and effective for this problem [12].
Before describing the algorithm, let us first address the necessary backgrounds on convex analysis and proximity operators [11].

3.3.1. Background on convex optimization tools

We denote by $\mathbb{R}^K$ the K-dimensional Euclidean space with norm $||\cdot||$. The main definitions which will be used in this work are the followings:

- The indicator function of a convex set $C \subset \mathbb{R}^K$ is given by :

$$\forall \mathbf{x} \in \mathbb{R}^K, \qquad \imath_C(\mathbf{x}) = \begin{cases} 0 & \text{if} \quad \mathbf{x} \in C, \\ +\infty & \text{otherwise.} \end{cases} \tag{10}$$

- The distance function to a nonempty set $C \subset \mathbb{R}^K$ is defined by:

$$\forall \mathbf{x} \in \mathbb{R}^K, \qquad d_C(\mathbf{x}) = \inf_{\mathbf{y} \in C} ||\mathbf{x} - \mathbf{y}||. \tag{11}$$

- The projection of $\mathbf{x} \in \mathbb{R}^K$ onto a nonempty closed convex set $C \subset \mathbb{R}^K$ is the unique point $P_C(\mathbf{x}) \in C$ such that $d_C(\mathbf{x}) = ||\mathbf{x} - P_C(\mathbf{x})||$.

- $\Gamma_0(\mathbb{R}^K)$ is the class of lower semicontinuous convex function from $\mathbb{R}^K$ to $]-\infty, +\infty]$ and not identically equal to $+\infty$.

- The proximity operator of a function $f \in \Gamma_0(\mathbb{R}^K)$, denoted by prox_f, is defined as follows:

$$\begin{aligned} \text{prox}_f : \ & \mathbb{R}^K \to \mathbb{R}^K \\ & \mathbf{x} \mapsto \underset{\mathbf{y} \in \mathbb{R}^K}{\arg\min}\ f(\mathbf{y}) + \frac{1}{2}||\mathbf{x} - \mathbf{y}||^2. \end{aligned} \tag{12}$$

3.3.2. Douglas-Rachford algorithm

In the following, the algorithm adopted to generate the residual image is described. We recall that the aim consists of minimizing the ℓ_1-norm of the difference between the current pixel of the right image $I^{(r)}(i,j)$ and its predicted value. In this context, the vector $\mathbf{I}^{(r)} = \Big(I^{(r)}(i,j)\Big)_{\substack{1 \le i \le W \\ 1 \le j \le H}}$ can be seen as an element of the Euclidean space $\mathbb{R}^{W \times H}$. The minimization problem (9) can be rewritten as follows:

$$\min_{\mathbf{X} \in V} \sum_{i=1}^{W} \sum_{j=1}^{H} |I^{(r)}(i,j) - X(i,j)|, \tag{13}$$

where $V = \{\mathbf{X} = \Big(X(i,j)\Big)_{\substack{1 \le i \le W \\ 1 \le j \le H}} | \ \exists\, \mathbf{p} \in \mathbb{R}^L,\ \forall (i,j) \in \{1,\dots,W\} \times \{1,\dots,H\},\ X(i,j) = \mathbf{p}^\top \mathbf{I}^{(c)}(i,j)\}$.

According to the definition of the indicator function (10), the minimization problem (13) is equivalent to the following one:

$$\min_{\mathbf{X} \in \mathbb{R}^{W \times H}} f_1(\mathbf{X}) + f_2(\mathbf{X}), \tag{14}$$

where

$$\begin{aligned} f_1(\mathbf{X}) =& ||\mathbf{I}^{(r)} - \mathbf{X}||_{\ell_1} \\ =& \sum_{i=1}^{W} \sum_{j=1}^{H} |I^{(r)}(i,j) - X(i,j)|, \end{aligned} \tag{15}$$

and

$$f_2(\mathbf{X}) = \imath_C(\mathbf{X}). \tag{16}$$

By writing it under this form, the minimization problem (14) can be solved by using the Douglas-Rachford algorithm. The obtained numerical solution can be obtained based on the following iterative algorithm :

Fix $\mathbf{S}_0 \in \mathbb{R}^{W \times H}$, $\gamma > 0$, $\epsilon \in]0,1[$ and $\lambda \in [\epsilon, 2-\epsilon]$
for $k = 0, 1, \dots$ **do**
  $\mathbf{X}_k = \text{prox}_{\gamma f_2} \mathbf{S}_k$,
  $\mathbf{S}_{k+1} = \mathbf{S}_k + \lambda\big(\text{prox}_{\gamma f_1}(2\mathbf{X}_k - \mathbf{S}_k) - \mathbf{X}_k\big)$.
end

Algorithm 1: Douglas-Rachford algorithm.

As it can be seen in this algorithm, each iteration requires the computation of two proximity operators for the functions f_1 and f_2. Note that closed-form expressions of the proximity operator of some functions belonging to $\Gamma_0(\mathbb{R}^K)$ are developed in [11].
In our case, the proximity operator of the function γf_1 is given by :

$$\forall \mathbf{S}_k \in \mathbb{R}^{W \times H}, \quad \text{prox}_{\gamma f_1}(\mathbf{S}_k) = \big(\pi_k(i,j)\big)_{\substack{1 \le i \le W, \\ 1 \le j \le H}} \tag{17}$$

where $\forall (i,j) \in \{1,\dots,W\} \times \{1,\dots,H\}$,

$$\pi_k(i,j) = \text{soft}_{[-\lambda,\lambda]}\big(S_k(i,j) - I^{(r)}(i,j)\big) + I^{(r)}(i,j) \tag{18}$$

and $\forall t \in \mathbb{R}$,

$$\text{soft}_{[-\lambda,\lambda]}(t) = \begin{cases} \text{sign}(t)(|t| - \gamma) & \text{if} \quad |t| > \gamma \\ 0 & \text{otherwise.} \end{cases} \tag{19}$$

Concerning γf_2, the proximity operator is given by:

$$\forall \mathbf{S}_k \in \mathbb{R}^{W\times H}, \qquad \begin{aligned} \text{prox}_{\gamma f_2}(\mathbf{S}_k) &= P_V(\mathbf{S}_k) \\ &= \left(\mathbf{p}^\top \mathbf{I}^{(c)}(i,j)\right)_{\substack{1\leq i\leq W,\\ 1\leq j\leq H}} \end{aligned} \tag{20}$$

where
$\mathbf{p} = \left(\sum_{i,j} \mathbf{I}^{(c)}(i,j)\mathbf{I}^{(c)}(i,j)^\top\right)^{-1} \sum_{i,j} S_k(i,j)\mathbf{I}^{(c)}(i,j)$.
Finally, we should note that it has been shown in [13] that every sequence $\mathbf{X}_k$ generated by the Douglas-Rachford algorithm converges to a solution to problem (14) if the selected parameters λ and γ satisfy the conditions given in Algorithm 1.

4. EXPERIMENTAL RESULTS

The simulations are performed on different standard stereo images downloaded from some public stereovision datasets [1, 2 and 3]. A block-matching technique with a 8×8 block size is employed to estimate firstly the disparity map. The latter is then losslessly encoded by using a DPCM technique followed by an arithmetic coder. Finally, to encode the reference image as well the residual one, the 9/7 (resp. 5/3) wavelet transform, retained for the lossy (resp. lossless) compression mode of JPEG2000 [14], is applied over three resolution levels. The resulting wavelet coefficients are then encoded by using the entropy coder EBCOT.
In order to study the proposed optimization strategies, we focus on the generation of the residual image by considering the three following experiments:

① The first one uses the standard computation procedure defined by Eq. (2). We refer to this method by "Standard".

② The second one consists of applying a weighting term as given by Eq. (3). The weight is computed by minimizing the variance of the residual coefficients. This method will be denoted by "Weighted-version".

③ The third and the fourth ones correspond to the proposed optimization strategies. More precisely, according to the notations used in Eq. (5), the pixels taken during the disparity compensation process are obtained by setting $m \in \{-1, 0, 1\}$ and $n \in \{-1, 0, 1\}$. The optimization based on the ℓ_2 and ℓ_1 criteria will be designated by "Proposed-ℓ_2-OPT" and "Proposed-ℓ_1-OPT", respectively.

In addition to these methods, we have also considered the independent coding scheme, denoted by "Independent", where the retained wavelet transform is applied separately to the left and right images.
First, the performance of these different methods will be evaluated in the context of lossless coding mode. Since the reference image is encoded in the same way for all the tested methods, we give in Table 1 the entropy of the multiresolution representations of the target image. The advantages of such measure are that it is easily computed and it is independent of the performance of any embedded coder. Compared to the standard approach, the proposed optimized computation strategy of the residual image results in a gain which can reach 0.25 bits per pixel (bpp). It can be also observed that the ℓ_1 optimization technique achieves a further improvement compared to the ℓ_2 optimization approach.

Table 1: Results in terms of entropy (in bpp) of the target images for the considered methods.

SI	Shrub	Art	Cones	Drumsticks
Independent	4.95	4.38	5.39	4.49
Standard	3.73	3.51	4.27	3.88
Weighted-version	3.70	3.51	4.26	3.87
Proposed-ℓ_2-OPT	3.39	3.51	4.22	3.88
Proposed-ℓ_1-OPT	3.37	3.46	4.19	3.83

Moreover, these methods have also been evaluated in the context of lossy coding mode. Note that a closed loop-based coding structure has been employed [5]. The reported results are given in terms of the average bitrate R_{av} and its corresponding PSNR measure:

$$R_{\text{av}} = \frac{R^{(l)} + R^{(e)} + R^{(d)}}{2}, \tag{21}$$

$$\text{PSNR} = 10\log_{10}\frac{255^2}{(\text{MSE}^{(l)} + \text{MSE}^{(r)})/2}, \tag{22}$$

where $R^{(l)}$, $R^{(e)}$ and $R^{(d)}$ denote respectively the bitrate of the left, target, and disparity images. $\text{MSE}^{(l)}$ and $\text{MSE}^{(r)}$ correspond respectively to the mean squared error of the reconstructed left and right images. Figure 1 illustrates the performance of the different considered stereo images compression methods for the stereo image "Shrub" and "Houseof". It can be observed that the proposed strategy outperforms the standard computation procedure by about 0.3-1 dB. Furthermore, we have also compared the ℓ_1-based optimization technique to the standard one in terms of Bjontegaard metric, often used to measure the distance between two R-D curves [15]. The PSNR differences and the bitrate saving between these two approaches are provided in Table 2 for low, middle and high bitrates corresponding to the four target bitrate points $\{0.15, 0.2, 0.3, 0.4\}$, $\{0.5, 0.6, 0.7, 0.8\}$ and $\{0.9, 1, 1.1, 1.2\}$ bpp, respectively. This table shows that the average of the PSNR differences between the R-D results varies between 0.14-1.2 dB.
Finally, we illustrate in Fig. 2 the reconstructed "Pentagon" stereo image. The reconstruction quality is evaluated in

[1] http://vision.middlebury.edu/stereo/
[2] http://vasc.ri.cmu.edu/idb/html/stereo/index.html
[3] http://vasc.ri.cmu.edu/idb/html/jisct/

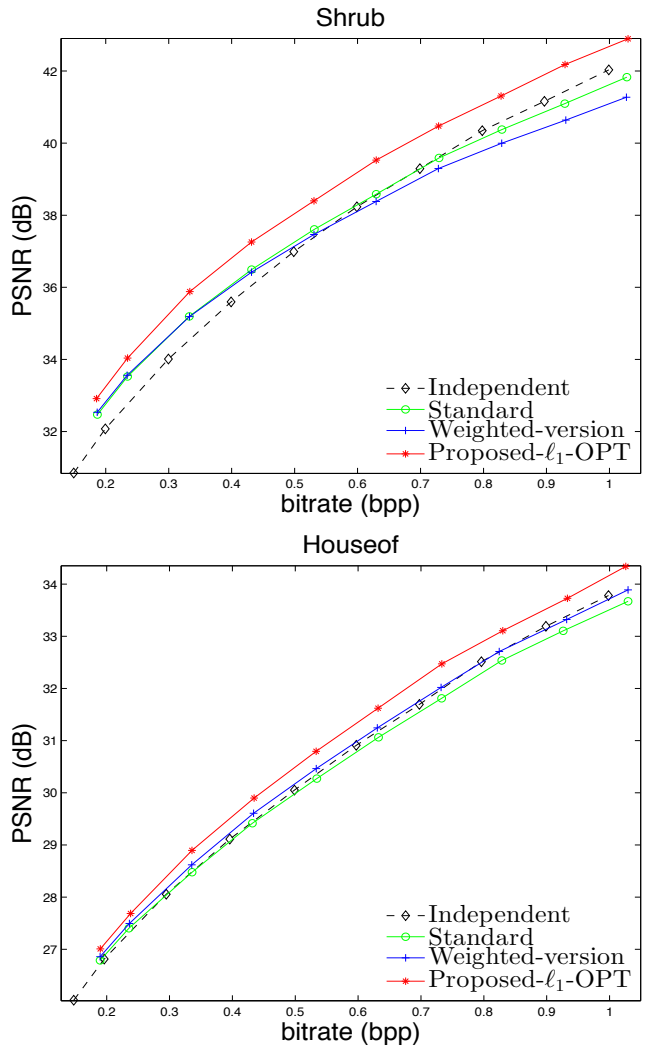

Fig. 1: PSNR (in dB) versus the bitrate (bpp) after JPEG 2000 encoding for the stereo images "Shrub" and "Houseof".

terms of PSNR. As it can be seen in Fig. 2, the proposed ℓ_1 optimization strategy leads to better reconstruction quality compared to the standard approach.
All these results confirm the benefits which can be drawn from the proposed techniques for optimizing the residual image.

5. CONCLUSION

In this work, we have focused on the optimization of the residual image to improve the stereo coding performance. More precisely, for each pixel in the target image, we have proposed to use the homologous pixel in the reference image as well its neighboring to generate the residual image. To this end, two optimization techniques including the ℓ_2 and ℓ_1 criteria have been investigated. Experimental results show the interest of this procedure in the design of a residual-based stereo coding scheme. While the developed optimization strategy is performed by using a criterion defined in the spatial domain, it would be interesting to investigate in future a more sophisticated criterion defined on the whole multiresolution representation of the residual image.

Table 2: The average PSNR differences and the bitrate saving at low, middle and high bitrates for different Stereo images. The gain of the Proposed ℓ_1-OPT method w.r.t to the standard one.

SI	PSNR gain (dB)			Bitrate saving (%)		
	low	middle	high	low	middle	high
Shrub	0.60	0.91	1.07	-11.97	-14.04	-13.81
Houseof	0.34	0.59	0.72	-10.19	-11.31	-10.80
Pentagon	0.52	0.91	1.20	-14.89	-16.92	-17.36
Art	0.22	0.24	0.25	-4.14	-3.42	-3.01
Cones	0.14	0.27	0.35	-3.42	-4.85	-4.49
Average	0.37	0.58	0.72	-8.92	-10.11	-9.89

6. REFERENCES

[1] M. E. Lukacs, "Predictive coding of multi-viewpoint image sets," in *IEEE International Conference on Acoustics Speech and Signal Processing*, Tokyo, Japan, 1986, pp. 521–524.

[2] M. G. Perkins, "Data compression of stereopairs," *IEEE Transactions on Communications*, vol. 40, no. 4, pp. 684–696, 1992.

[3] W. Hachicha, A. Beghdadi, and F. A Cheikh, "1D directional DCT-based stereo residual compression," in *European signal Processing Conference*, Marrakech, Morocco, 2013.

[4] M. S. Moellenhoff and M. W. Maier, "Transform coding of stereo image residuals," *IEEE Transactions on Image Processing*, vol. 7, no. 6, pp. 804–812, June 1998.

[5] N. V. Boulgouris and M. G. Strintzis, "A family of wavelet-based stereo image coders," *IEEE Transactions on Circuits and Systems for Video Technology*, vol. 12, no. 10, pp. 898–903, 2002.

[6] M. Kaaniche, A. Benazza-Benyahia, B. Pesquet-Popescu, and J-C. Pesquet, "Vector lifting schemes for stereo image coding," *IEEE Transactions on Image Processing*, vol. 18, no. 11, pp. 2463–2475, 2009.

[7] M. Kaaniche, B. Pesquet-Popescu, A. Benazza-Benyahia, and J.-C. Pesquet, "Adaptive lifting scheme with sparse criteria for image coding," *EURASIP Journal on Advances in Signal Processing: Special Issue on*

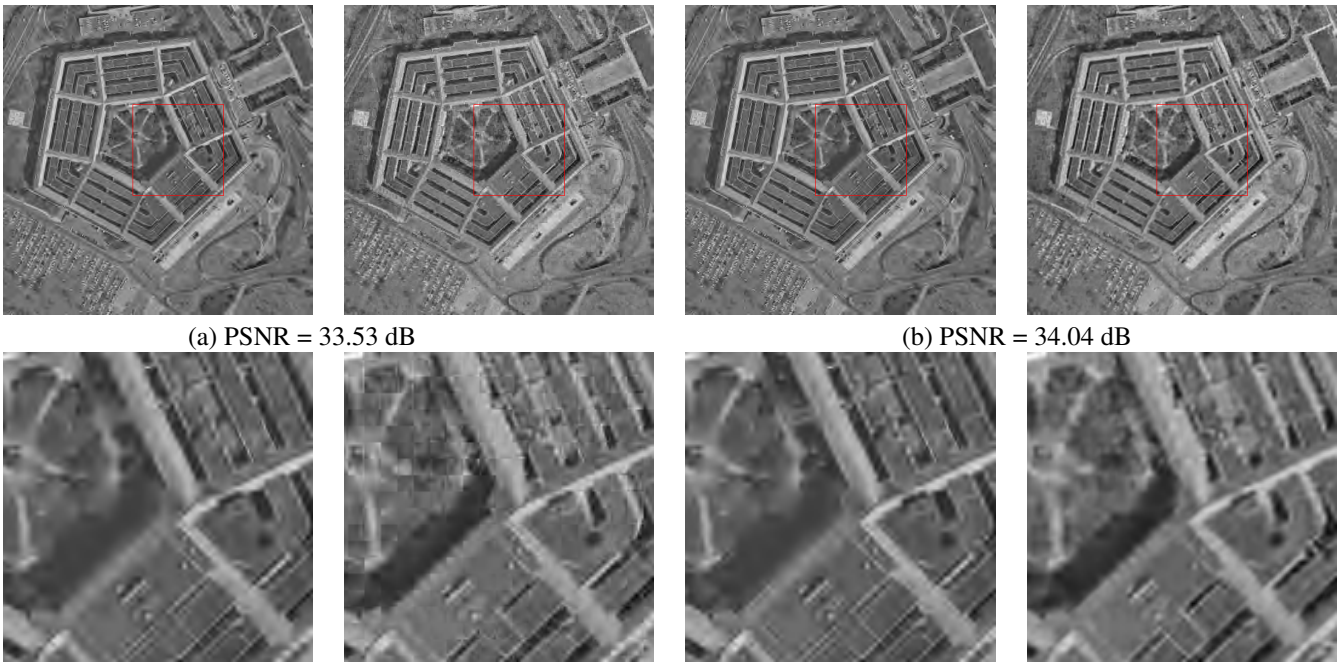

(a) PSNR = 33.53 dB (b) PSNR = 34.04 dB

Fig. 2: Reconstructed "Pentagon" stereo image coded at R_{av}=0.23 bpp, (a) Standard and (b) Proposed-ℓ_1-OPT.

New Image and Video Armentiéroises Based on Sparsity, vol. 2012, 22 pages, January 2012.

[8] D. Scharstein and R. Szeliski, "A taxonomy and evaluation of dense two-frame stereo correspondence algorithms," *International journal of computer vision*, vol. 47, no. 1-3, pp. 7–42, 2002.

[9] W. Miled, J.-C. Pesquet, and M. Parent, "A convex optimization approach for depth estimation under illumination variation," *IEEE Transactions on Image Processing*, vol. 18, no. 4, pp. 813–830, 2009.

[10] D.L. Donoho, "Compressed sensing," *IEEE Transactions on Information Theory*, vol. 52, no. 4, pp. 1289–1306, 2006.

[11] P.L. Combettes and J-C. Pesquet, "Proximal splitting methods in signal processing," *Fixed-Point Algorithms for Inverse Problems in Science and Engineering*, p. 185, 2010.

[12] J. Eckstein and D.P. Bertsekas, "On the douglas-rachford splitting method and the proximal point algorithm for maximal monotone operators," *Mathematical Programming*, vol. 55, no. 1-3, pp. 293–318, 1992.

[13] P.L. Combettes and J-C. Pesquet, "A Douglas-Rachford splitting approach to nonsmooth convex variational signal recovery," *IEEE Journal of Selected Topics in Signal Processing*, vol. 1, no. 4, pp. 564–574, 2007.

[14] D. Taubman and M. Marcellin, *JPEG2000: Image Compression Fundamentals, Standards and Practice*, Kluwer Academic Publishers, Norwell, MA, USA, 2001.

[15] G. Bjontegaard, "Calculation of average PSNR differences between RD curves," Tech. Rep., ITU SG16 VCEG-M33, Austin, TX, USA, April 2001.